RSC Advances

PAPER

View Article Online
View Journal | View Issue

Cite this: *RSC Adv.*, 2021, **11**, 2383

Nanoparticles with PDT and PTT synergistic properties working with dual NIR-light source simultaneously†

Fazli Sozmen, *[a] Merve Kucukoflaz,[a] Mustafa Ergul[b] and Zeynep Deniz Sahin Inan[c]

Received 24th November 2020
Accepted 2nd January 2021

DOI: 10.1039/d0ra09954f

rsc.li/rsc-advances

A non-toxic nano system using a cleverly designed dual light can be an important treatment strategy in cancer therapy. Here, we propose a unique concept of synergistic non-toxic nanoplatform, which operates with dual light. An apoferritin nano-platform whose surface was modified with Verteporfin (Visudyne®) and with ultra-small CuS nanoparticles in the center demonstrated the synergistic effect of photodynamic therapy (PDT) and photothermal therapy (PTT). The synergistic effect of PDT and PTT were achieved with 808 nm laser light and 690 nm LED light, respectively. These results not only give a new horizon to multifunctional nanostructures for biological applications but also show a new way to design the novel PDT and PTT agents.

1. Introduction

As is known to all, cancer is one of the most dangerous and deadly diseases of today. In addition to surgical intervention, chemotherapy is still the leading method used in cancer treatment. However, the drugs used in chemotherapy are still not at the desired point in terms of their side effects.[1] Therefore, drug designs with targeted and fewer side effects come to the fore. Choosing a treatment method according to cancer type and location have become necessary in cancer treatment. While making this choice, it has become increasingly important to develop personalized treatment methods to find the most effective and least side effect method.[2,3] In this regard, photodynamic and photothermal therapies have become the focus of increasing interest.[4,5] In both photodynamic therapy (PDT) and photothermal therapy (PTT), the place where radiation is applied is generally targeted, and therefore no extra targeting is often needed. One of the main problems in these two therapy methods is tissue penetration of light. In PDT and PTT therapies, issues such as the formation of a hypoxic environment and the heat conversion efficiency of light are the other main problems, respectively.[6,7] For such reasons, synergistic strategies are becoming increasingly important.[8,9] Thus, problems will be overcome with a synergistic approach and a better result will be obtained from the effects they have on their own.

Ferritin nanoparticles are highly suitable platforms for biology applications as they are protein-based structures and serve as iron storage units in most living organisms.[10,11] While the internal cavities of apoferritin (**Afrt**) nanoparticles obtained from demineralization of ferritin nanoparticles are used to encapsulate various molecules for applications such as biological imaging, drug release, their outer surfaces are usually functionalized with various biological agents for purposes such as targeting.[12–14]

Gold nanoparticles are the leading nanoparticles used in PTT.[15–17] However, copper sulfide (CuS) nanoparticles have also been frequently used in recent studies on PTT.[18–20] Wang *et al.* achieved to synthesize ultrasmall CuS nanoparticles inside the cavity of **Afrt** nanocages by a biomimetic synthesis method.[21] These nanocages showed strong near-infrared absorbance and high photothermal conversion efficiency.

Verteporfin (**VP**) is a photosensitizer that produces singlet oxygen when excited with a 690 nm LED light that has been clinically approved for the treatment of acute macular degeneration.[22] The efficient singlet oxygen generation ability makes **VP** a good candidate as a PDT agent in cancer treatment and several studies are also available.[23–25] In this study, we aimed to synthesize **Afrt** nanoparticles whose surfaces are functionalized with **VP** and have ultra-small copper sulfide (CuS) nanoparticles in their inner cavity. Thus, while these nanoparticles acted as PTT agents by absorbing 808 nm laser light by ultra-small CuS nanoparticles, they also showed a PDT effect with **VP** photosensitizer *via* absorption of 690 nm LED light. As a consequence, using two different wavelength lights, we synergistically combined PTT and PDT therapies in a single nanoplatform, and in doing so we used biocompatible **Afrt** nanocages as scaffolds. To the best of our knowledge, there is as yet no example of a **VP**,

[a]*Nanotechnology Engineering Department, Faculty of Engineering, Sivas Cumhuriyet University, 58140, Sivas, Turkey. E-mail: fsozmen@cumhuriyet.edu.tr*

[b]*Biochemistry Department, Faculty of Pharmacy, Sivas Cumhuriyet University, 58140, Sivas, Turkey*

[c]*Histology and Embryology Department, Faculty of Medicine, Sivas Cumhuriyet University, 58140, Sivas, Turkey*

† Electronic supplementary information (ESI) available. See DOI: 10.1039/d0ra09954f

Afrt, CuS nanoplatform which has a dual NIR-light PDT and PTT synergistic effect.

2. Results and discussion

The study started with the synthesis of **Afrt-CuS** nanoparticles with ultra-small CuS nanoparticles in the internal cavity. These nanoparticles have been successfully synthesized before by Wang *et al.*[21] One of the main reasons why **Afrt** nanoparticles are chosen both as encapsulating CuS nanoparticles and as a surface provider for binding of **VP** is that it shows good tumor uptake. Light-induced heat generation ability makes CuS nanoparticles a good option for the PTT, however, often PTT or PDT may not be able to exert the effect expected of them alone.[6] Therefore, in our design, we first encapsulated the CuS nanoparticles with **Afrt** nanoparticles, then we functionalized the surfaces of these nanoparticles with a PDT agent, **VP**. Thus, nanoparticles with both PDT and PTT effects were obtained on the apoferritin nanoplatform and 808 nm (1.5 W cm^{-2}) laser and 690 nm LED light sources were used simultaneously to activate these nanoparticles (Fig. 1).

Initially, **VP-NHS** (verteporfin succinimidyl ester) was synthesized *via* the transformation of the carboxyl group present on the **VP** into *N*-hydroxysuccinimide ester using NHS/DCC coupling reaction (Fig. S4†). Then the surface lysines of **Afrt** nanocages were utilized for the functionalization of surfaces of **Afrt-CuS** nanoparticles with **VP** (Fig. 2). The size distribution of **Afrt-CuS** nanoparticles and **VP-Afrt-CuS** nanoparticles was measured from dynamic light scattering (DLS) analysis, with average diameters of 12.3 nm and 83.8 nm, respectively, indicated a slight increase in size after **VP** functionalization of **Afrt-CuS** nanoparticles (Fig. S1† and Fig. 2b). Additionally, their zeta potentials have been found as −42.6 mV and −32.9 mV (pH = 7.0) respectively (Fig. S2 and S7†). A slight aggregation was observed in SEM images for both **Afrt-CuS** and **VP-Afrt-CuS** nanoparticles (Fig. 2a and Fig. S3†)

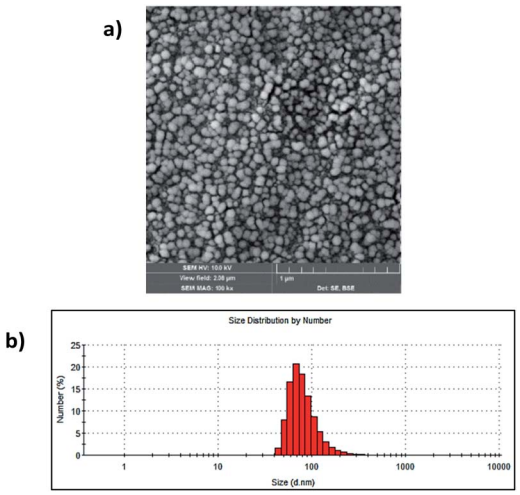

Fig. 2 (a) SEM image of **VP-Afrt-CuS** nanoparticles stained with 2% uranyl acetate. (b) The size distribution of **VP-Afrt-CuS** nanoparticles.

To assess the PDT effect of **VP-Afrt-CuS** nanoparticles, 1,3-diphenylisobenzofuran (DPBF) was used as a singlet oxygen trap and **VP-Afrt-CuS** nanoparticles were first exposed to 690 nm LED light in the presence of trap molecule in DMSO. During the irradiation with the LED lamp, the decrease in the absorbance of the trap molecule was monitored (Fig. 3b). The same measurement was then repeated using an 808 nm (1.5 W cm^{-2}) laser instead of a LED lamp (Fig. 3a). Finally, the measurement was repeated by simultaneously exposing the **VP-Afrt-CuS** nanoparticles to the 808 nm (1.5 W cm^{-2}) laser and 690 nm LED light (Fig. 3c). As we expected, due to the **VP** molecules present on the surfaces of the **VP-Afrt-CuS** nanoparticles, these nanoparticles showed good singlet oxygen production properties when exposed to only 690 nm LED light and both 808 nm (1.5 W cm^{-2}) laser and 690 nm LED light, and the results were close to each other. However, **VP-Afrt-CuS** nanoparticles exposed only to

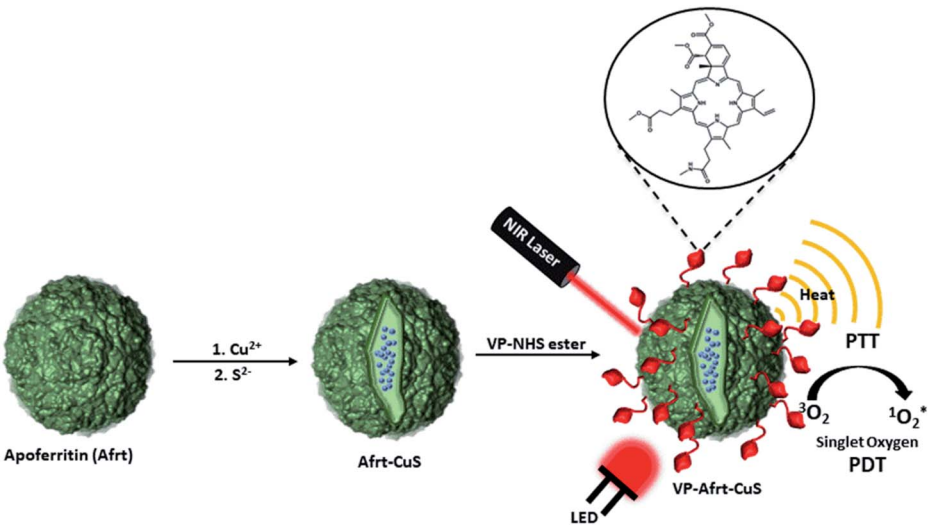

Fig. 1 Synthesis and working principle of **VP-Afrt-CuS** nanoparticles. First, **Afrt-CuS** nanoparticles have been synthesized with ultra-small CuS nanoparticles in the internal cavity. Second, the surface of **Afrt-CuS** nanoparticles has been functionalized with **VP**. 808 nm (1.5 W cm^{-2}) laser and 690 nm LED have been used to obtain synergistic features of PTT and PDT.

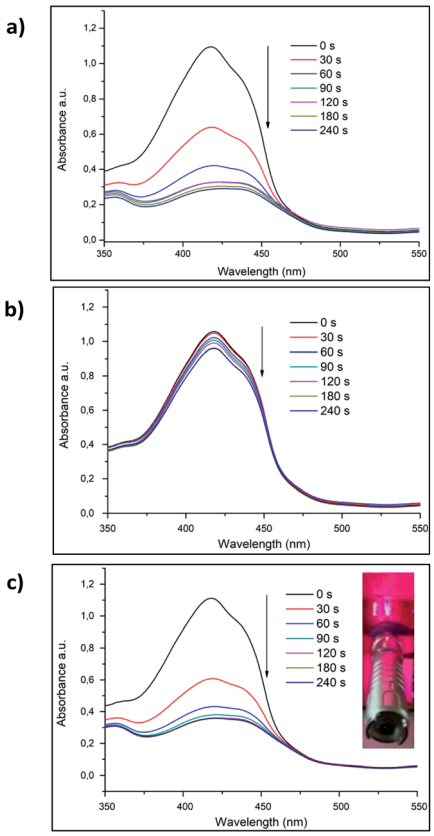

Fig. 3 (a) Decrease in the absorbance of DPBF in the presence of 22.5 mg mL^{-1} **VP-Afrt-CuS** nanoparticles (total volume 250 μL) at 416 nm in DMSO after irradiated with 690 nm LED. (b) Decrease in the absorbance of DPBF in the presence of 22.5 mg mL^{-1} **VP-Afrt-CuS** nanoparticles (total volume 250 μL) at 416 nm in DMSO after irradiated with 808 nm (1.5 W cm^{-2}) laser. (c) Decrease in the absorbance of DPBF in the presence of 22.5 mg mL^{-1} **VP-Afrt-CuS** nanoparticles (total volume 250 μL) at 416 nm in DMSO after irradiated with 808 nm (1.5 W cm^{-2}) laser and 690 nm LED, simultaneously. Inset: irradiation of **VP-Afrt-CuS** nanoparticles with 808 nm (1.5 W cm^{-2}) laser and 690 nm LED, simultaneously.

808 nm (1.5 W cm^{-2}) laser light produced much less singlet oxygen, since the maximum absorbance of **VP** was 690 nm.

As for the PTT properties of the **VP-Afrt-CuS** nanoparticles, the nanoparticles were first exposed to only 808 nm (1.5 W cm^{-2}) laser light at different times in PBS (pH = 7.4), and the temperature changes in the solution were monitored with a thermal camera (Testo IR) (Fig. 4). Once the results are compared with temperature changes of PBS solution, **VP-Afrt-CuS** nanoparticles were significantly more heated when exposed to 808 nm (1.5 W cm^{-2}) laser light. The nanoparticles were exposed to 690 nm LED lamp alone, but this lamp did not show any PTT property. Accordingly, **VP-Afrt-CuS** nanoparticles have an apparent PTT feature. Thus, by individual experiments, it was understood that **VP-Afrt-CuS** nanoparticles have both PDT and PTT properties at 690 nm and 808 nm wavelength lights, respectively.

In the current study, **VP-Afrt-CuS** nanoparticles (with or without LED and laser) has been assessed for their cytotoxicity in MDA-MB-231 cells. The cells were treated with different

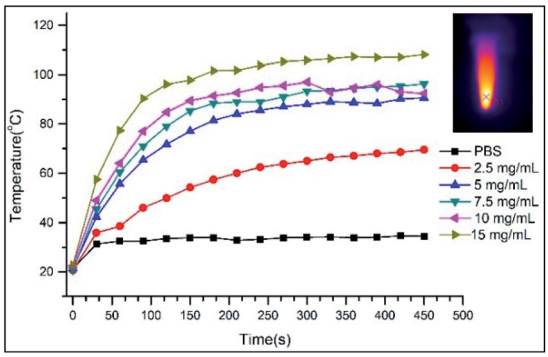

Fig. 4 Temperature increase of **VP-Afrt-CuS** nanoparticles at different concentrations in PBS (pH = 7.4) after irradiation with 808 nm (1.5 W cm^{-2}) laser for various times. Inset: thermal camera image of **VP-Afrt-CuS** nanoparticles (10 mg mL^{-1}) after irradiation with 808 nm (1.5 W cm^{-2}) laser for 450 second.

concentrations of **VP-Afrt-CuS** solutions and cytotoxicity was determined using the XTT assay. As shown in Fig. 5a, no cytotoxicity was observed in the **VP-Afrt-CuS** nanoparticles only group. However, after the treatment of **VP-Afrt-CuS** nanoparticles, LED or laser irradiation significantly decreased cell viability in a concentration-dependent manner. As expected, combined irradiation of LED and laser resulted in higher cytotoxicity when compared with LED or laser alone.

To evaluate whether **VP-Afrt-CuS** nanoparticles exhibit selective cytotoxicity between normal and cancer cells, L929 cells were exposed to **VP-Afrt-CuS** at 0.5–10 μM concentrations

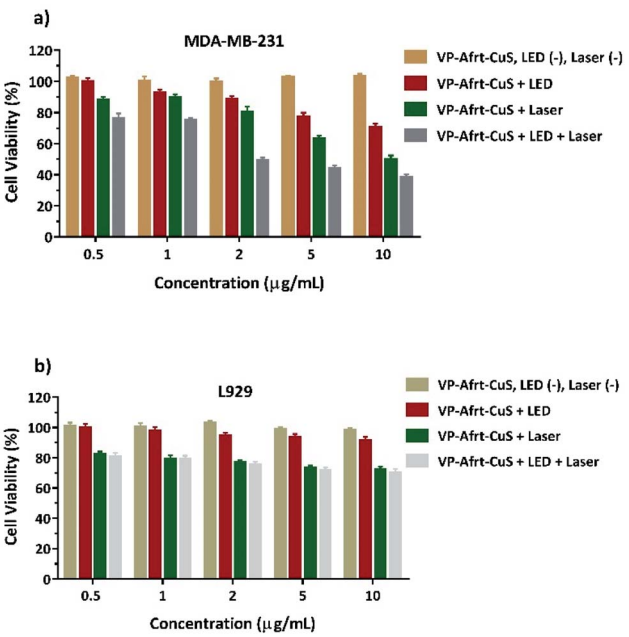

Fig. 5 *In vitro* cytotoxicity experiments. Relative viability of MDA-MB-231 (a) and L929 (b) cells incubated with various concentrations of **VP-Afrt-CuS** nanoparticles for 24 h with or without irradiation by LED, laser, or LED + laser. Cell viability was examined using the XTT assay and results are expressed as mean ± SD in triplicate.

for 24 h. XTT data revealed that while **VP-Afrt-CuS** nanoparticles alone did not show any cytotoxicity, especially laser irradiation and combined application of LED and laser showed moderately cytotoxic activity against L929 cells when compared to the cancer cells (Fig. 5b). This data suggested that **VP-Afrt-CuS** nanoparticles alone, with LED or with LED and laser have a significantly low cytotoxic effect towards the L929 cells may have importance in preventing severe side effects in cancer treatment.

Moreover, the total oxidant status (TOS) is among the diverse parameters used in the estimation of oxidative stress and it is frequently used to evaluate the overall oxidation state of the body.[26] In light of these data, the effect of **VP-Afrt-CuS** nanoparticles on TOS of MDA-MB-231 cells was determined using the TOS assay kit. TOS values were calculated as 1.79 ± 0.76%, 1.91 ± 0.91, 2.33 ± 1.01, 2.88 ± 0.77, 13.21 ± 0.98, 3.08 ± 1.11, and 14.3 ± 0.45 in control, control LED, control laser, control LED + laser, **VP-Afrt-CuS** LED, **VP-Afrt-CuS** laser, and **VP-Afrt-CuS** LED + laser groups, respectively (Fig. 6). These results revealed that **VP-Afrt-CuS** treatment following LED or LED + laser irradiation significantly increased TOS levels in MDA-MB-231 cells supporting their cytotoxic effects. These data are also confirmed the PDT experiments.

TUNEL (terminal deoxynucleotidyl transferase-mediated dUTP notch end labeling) is the preferred and frequently used method for rapid identification and quantification of apoptotic cell fraction in cultured cell preparations.[27] Apoptosis, called programmed cell death, is a selective process that occurs to maintain homeostasis during normal and abnormal processes. In cancer research, it is essential to selectively destroy cancer cells, protect healthy cells, and lack an inflammatory response. Therefore, demonstrating apoptotic cancer cells in studies adds value to anticancer treatment approaches.[28,29] In this study, TUNEL stained cells in the cell fraction with and without apoptotic morphology were marked. Thus, it was aimed to determine the effectiveness of the **VP-Afrt-CuS** nanoparticles used in the MDA-MB-231 cancer cell line. MDA-MB-231 cells (10×10^5 cells per well) were grown on 6-well plates in the medium previously described.[30,31] The cells were incubated for 24 h after a, b, c, d, e, f, g procedures, and they were photographed under a light microscope at the end of the incubation (Fig. 7, a–g bright field (BF)). In the light microscopy photographs, non-apoptosis-resistant MDA-MB-231 cells show smooth cell membrane, cytoplasm, and nuclear membrane morphology similar to those in the group a, while groups of cells undergoing apoptosis are observed as dark black and small cells. It is observed in the morphological structure characterized by an increasing number of nuclei clusters in groups b, c, d, e, f, and g. Twenty-four hours after processing the cells, TdT-mediated dUTP X notch end labeling (TUNEL) positive cells were identified by *In Situ* Cell Death Detection Kit, Fluorescein (Roche, Sigma Aldrich; Merck KGaA) according to the manufacturer's instructions. The cell image was photographed using a fluorescence microscope after counterstaining with 1 μg mL^{-1} 4′,6-diamidino-2-fenilindol (DAPI) dye.

With TUNEL/DAPI double staining, apoptotic cells appear with green fluorescent staining, and cell nuclei appear in blue fluorescence with DAPI staining. As seen in Fig. 7, in the group a, few cells appear apoptotic and nuclear morphology begins to deteriorate. Apoptotic cells gradually increase in groups b, c, d, the increase is greater in groups e and f, and apoptosis is observed in many cells in group g. Based on *in vitro* experiments with MDA-MB-231 breast cancer cells, most apoptosis was detected in group g, where laser and LED were used together. This result supports that LED and laser have synergistic effects together, and PDT and PTT occur at the same time.

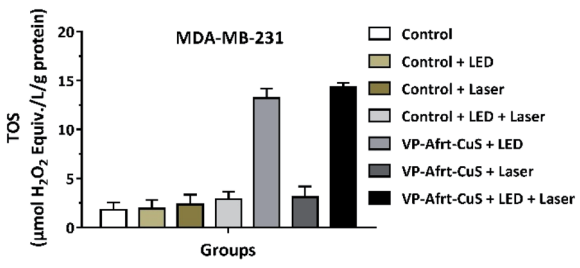

Fig. 6 LED, laser, and LED + laser irradiation following **VP-Afrt-CuS** treatment increased the total oxidant status (TOS) of MDA-MB-231 cells. Values are mean ± SD of three samples of the medium from wells containing MDA-MB-231 cells.

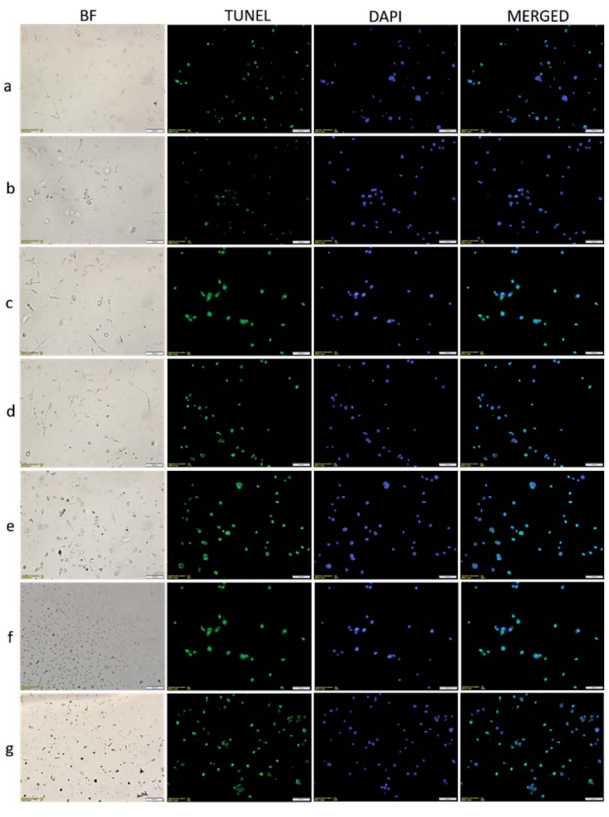

Fig. 7 MDA-MB-231 cells were treated with different concentrations of **VP-Afrt-CuS** nanoparticles and irradiated NIR laser (808 nm, 1.5 W cm^{-2}) and/or LED lamp (690 nm) for various times. (a) Control group, (b) control group + 690 nm LED (3 min), (c) control group + 808 nm laser (1 min), (d) control group + 690 nm LED (3 min) + 808 nm laser (1 min), (e) **VP-Afrt-CuS** NPs + 808 nm laser (1 min), (f) **VP-Afrt-CuS** NPs + 690 nm LED (3 min), (g) **VP-Afrt-CuS** NPs + 808 nm laser (1 min) + 690 nm LED (3 min).

3. Conclusions

In summary, we have successfully described an **Afrt** and CuS based nanoplatform with a useful PTT and PDT synergistic effect. Accordingly, for the PTT feature, **Afrt-CuS** nanoparticles were synthesized by forming CuS nanoparticles in the inner cavities of the bio-based **Afrt** nanoparticles. Then, for PDT feature, the outer surfaces of **Afrt-CuS** nanoparticles were functionalized with **VP**. Thus, these two features were obtained simultaneously with two different light sources. More importantly, the synergistic effect of PDT and PTT was achieved on a biologically based nanoplatform.

The present work not only shows the synthesis of rationally designed new nanoplatform but it also inspires novel nanomaterials working with the dual light source. So these nanoparticles have great potential especially for the treatment of melanoma or cancer types just below the skin. The outcomes from this study will be extremely useful for PDT and PTT used in clinical medical applications and cancer therapy.

4. Experimental

4.1 Synthesis of VP-NHS ester

VP-NHS ester was prepared as described by Kuimova *et al.* with slight modification.[22] *N*-Hydroxysuccinimide (6 mg, 0.0522 mmol) and DCC (12 mg, 0.0582 mmol) were added to the solution of Verteporfin (12 mg, 0.0168 mmol) in anhydrous THF (7 mL) respectively. The reaction mixture was stirred overnight under argon and then it was evaporated. The residue was purified by column chromatography on silica gel using ethyl acetate as mobile phase ($R_f = 0.74$, 70%).

4.2 Synthesis of Afrt-CuS nanoparticles

Afrt-CuS nanoparticles were also synthesized according to literature with slight modification.[21] 250 μL, 25 mM copper(II) chloride solution was added to 0.5 mL, 1 mg mL^{-1} apoferritin solution and stirred for 20 min at room temperature. Then the mixture was purified by filtration through a 10 kDa cutoff filter. The 0.1% sodium acetate solution was used as eluent. After that, 0.25 mL, 25 mM Na_2S solution was added to this purified solution and stirred at 60 °C for 25 min. Then the mixture was transferred to an ice bath and waited for 20 min. After that, the product was purified with filtration through a 10 kDa cutoff filter and it was kept in the refrigerator at +4 °C for later use.

4.3 Synthesis of VP-Afrt-CuS nanoparticles

VP-Afrt-CuS nanoparticles were prepared by conjugation of the **VP-NHS** ester to the surface lysine of the **Afrt-CuS** nanoparticles. In brief, **VP-NHS** ester solution (1 mg in 75 μL DMSO) was added to the solution of 10 mg **Afrt-CuS** nanoparticles in 1 mL PBS (pH 7.4) and the mixture was gently stirred for three hours at room temperature. Then the mixture was passed through a NAP-5 column to get rid of unreacted **VP-NHS** ester. After that the product was further purified with filtration through a 10 kDa cutoff, and redissolved in the ultrapure water with sonication for use.

4.4 Determination of PDT properties of VP-Afrt-CuS nanoparticles

For the determination of PDT properties of **VP-Afrt-CuS** nanoparticles, 1,3-diphenylisobenzofuran (DPBF) was used as a singlet oxygen trap molecule. For this purpose, after taking separate measurements with 808 nm (1.5 W cm^{-2}) laser and 690 nm LED lamp, the measurement was repeated using both light sources simultaneously. In a typical procedure used 808 nm (1.5 W cm^{-2}) laser as a light source, **VP-Afrt-CuS** nanoparticles and trap molecule were mixed in DMSO. Before laser irradiation, initially, several dark measurements were taken. Subsequently, the DMSO solution was exposed to 808 nm (1.5 W cm^{-2}) laser light at various times. Absorbance decrease of trap molecule was monitored suggesting singlet oxygen generation in the presence of light.

4.5 Determination of PTT properties of VP-Afrt-CuS nanoparticles

Since the LED lamp has no PTT effect on **VP-Afrt-CuS** nanoparticles, experiments were carried out using only 808 nm (1.5 W cm^{-2}) wavelength laser as the light source. So, PBS (pH = 7.4) solutions containing **VP-Afrt-CuS** nanoparticles at different concentrations were exposed to 808 nm (1.5 W cm^{-2}) laser light for various times, and temperature changes in PBS (pH = 7.4) solutions were monitored by a thermal camera (Testo IR). As a control experiment, only PBS (pH = 7.4) solution was exposed to laser light for various times and temperature changes were also monitored by a thermal camera.

4.6 Cell lines and cell culture

Human breast cancer cells MDA-MB-231 (HTB-26) and mouse fibroblast cells L929 (CRL-6364) were obtained from American Type Culture Collection (ATCC, USA). DMEM (Sigma-Aldrich) was used for the growth of MDA-MB-231 and L929 cells and it was supplemented with 10% Fetal Bovine Serum (FBS) (Gibco, Thermo Fisher Scientific), 1% L-glutamine (Sigma-Aldrich) and 1% penicillin/streptomycin (Gibco, Thermo Fisher Scientific) antibiotic mixtures. Cells were cultured at 37 °C within 5% CO_2 humidified atmosphere. **VP-Afrt-CuS** nanoparticles were dissolved in DMSO and it was further diluted with DMEM prior to treatment with a final percentage of DMSO less than 0.1%. The **VP-Afrt-CuS** nanoparticles-untreated cells were also exposed to DMEM containing 0.1% DMSO.

4.7 Cytotoxicity assay

Effect of different concentrations of **VP-Afrt-CuS** nanoparticles on MDA-MB-231 cell viability (after treatment with 690 nm LED, 808 nm (1.5 W cm^{-2}) laser or 690 nm LED + 808 nm (1.5 W cm^{-2}) laser) was evaluated the XTT (2,3-bis-(2-methoxy-4-nitro-5-sulfophenyl)-2*H*-tetrazolium-5-carboxanilide) assay (Roche). The cells were seeded in 96 well plates at a density of 1×10^4 cells per well in 100 μL DMEM culture media and later incubated overnight before treatment. The next day, the cells were treated with **VP-Afrt-CuS** nanoparticles at different concentrations (10, 5, 2, 1, 0.5 μg mL^{-1}) for 24 h. After incubation, the

media containing different concentrations of **VP-Afrt-CuS** nanoparticles were removed, the wells were washed twice with PBS and 100 μL of fresh DMEM was added to the wells. After laser and LED application ((690 nm LED (3 min), 808 nm (1.5 W cm^{-2}) laser (1 min) or 690 nm LED (3 min) + 808 nm (1.5 W cm^{-2}) laser (1 min)) the cells were incubated for another 24 h. The media containing different concentrations of **VP-Afrt-CuS** nanoparticles was then removed, the wells were washed twice with PBS and 100 μL of colorless DMEM plus 50 μL of XTT mixture solution was added to each well and incubated for 4 h. Finally, the absorbance was determined using an ELISA microplate reader (Thermo) at 450 nm and the cell viability was evaluated as a viable cell amount percent compared to control, as untreated cells.

4.8 Measurement of Total Oxidant Status (TOS)

TOS in different groups of cells was determined using the Total Oxidant Status Assay Kit (Rel Assay Diagnostics, Gaziantep, Turkey). MDA-MB-231 cells were treated with **VP-Afrt-CuS** nanoparticles and incubated for 24 h. After incubation, the media containing different concentrations of **VP-Afrt-CuS** nanoparticles were removed, the wells were washed twice with PBS and 3 mL of fresh DMEM was added to the wells. After that, laser, LED or laser + LED applications to the cells were performed and for measured the TOS in various groups manufacturer's protocol was followed. The results were presented in μmol H_2O_2 equivalent per L (μmol H_2O_2 equiv. per L).

4.9 Apoptosis study by fluorescence microscopy

The TUNEL (Roche, Germany) procedure applied in our study was carried out as specified by the manufacturer.[32,33] Briefly, MDA-MB-231 breast cancer cell line was seeded on sterile coverslips placed in 6-well plates at 10×10^4 cells each well. Groups were then formed as indicated in the "Total Oxidant Level (TOS) Measurement" section, and the cells were treated in the same way. The media on the coverslips was removed, washed twice with PBS, and air dry. Freshly prepared 4% paraformaldehyde/PBS (Sigma, Germany) was fixed at pH 7.4 at room temperature for 60 min and washed again with PBS. The cells were infused in freshly prepared Triton X-100 in 1% sodium citrate at 2–8 °C for 2 min. Negative controls were treated with 50 μL label solution. The enzyme solution in the kit was mixed with the label solution and incubated. Before applying the prepared mixture to the positive controls, 10 min in micrococcal nuclease or DNase 1 recombinant solution (50 mM Tris–HCL, pH 7.5, 3000 U/mL-3 U/mL in 1 mg mL^{-1} BSA) to detect DNA breaks was suspended. Cells that had been passed through PBS twice were then applied to each sample with 50 μL of TUNEL blend solution (label and enzyme solution mixture) and incubated at 37 °C in humid dark for 60 min. Groups were washed 3 times with PBS-Triton-X. The TUNEL was stained with 4′6′-diamidine-2-phenyl-indole dihydrochloride (DAPI) (200 nm mL^{-1}) for 5 min to observe core morphology after staining. The cells were rewashed with PBS-Triton-X 100 and examined under a fluorescence microscope. The coverslip we placed under the culture plate on the slide was carefully inverted (Olympus BX51 Japan). TUNEL staining of all groups was evaluated by making negative controls. In each groups, cells marked as apoptotic with TUNEL were scored twice by two different histologists; 3 areas were semi-quantitatively identified and photographed from appropriate areas.

Author contributions

The manuscript was written through contributions of all authors. All authors have given approval to the final version of the manuscript.

Conflicts of interest

The authors declare no conflict of interest.

Acknowledgements

The authors gratefully acknowledge support from TUBITAK (Grant No. 218Z053). The authors would like to thank the Sivas Cumhuriyet University Faculty of Medicine Research Center (CÜTFAM) for its technical support.

References

1 R. Oun, Y. E. Moussa and N. J. Wheate, The side effects of platinum-based chemotherapy drugs: a review for chemists, *Dalton Trans.*, 2018, **47**, 6635–6870.
2 K. Goutsouliak, J. Veeraraghavan, V. Sethunath, C. D. Angelis, C. K. Osborne, M. F. Rimawi and R. Schiff, Towards personalized treatment for early stage HER2-positive breast cancer, *Nat. Rev. Clin. Oncol.*, 2020, **17**, 233–250.
3 M. Verma, Personalized Medicine and Cancer, *J. Pers. Med.*, 2012, **2**, 1–14.
4 G. Lan, K. Ni, Z. Xu, S. S. Veroneau, Y. Song and W. Lin, Nanoscale Metal–Organic Framework Overcomes Hypoxia for Photodynamic Therapy Primed Cancer Immunotherapy, *J. Am. Chem. Soc.*, 2018, **140**, 5670–5673.
5 P. Yang, S. Zhang, N. Zhang, Y. Wang, J. Zhong, X. Sun, Y. Qi, X. Chen, Z. Li and Y. Li, Tailoring Synthetic Melanin Nanoparticles for Enhanced Photothermal Therapy, *ACS Appl. Mater. Interfaces*, 2019, **11**, 42671–42679.
6 S. Kolemen, T. Ozdemir, D. Lee, G. M. Kim, T. Karatas, J. Yoon and E. U. Akkaya, Remote-Controlled Release of Singlet Oxygen by the Plasmonic Heating of Endoperoxide-Modified Gold Nanorods: Towards a Paradigm Change in Photodynamic Therapy, *Angew. Chem.*, 2016, **128**, 3670–3674.
7 Q. Tian, F. Jiang, R. Zou, Q. Liu, Z. Chen, M. Zhu, S. Yang, J. Wang, J. Wang and J. Hu, Hydrophilic Cu9S5 Nanocrystals: A Photothermal Agent with a 25.7% Heat Conversion Efficiency for Photothermal Ablation of Cancer Cells in Vivo, *ACS Nano*, 2011, **5**, 9761–9771.
8 X. Yan, H. Hu, J. Lin, A. J. Jin, G. Niu, S. Zhang, P. Huang, B. Shen and X. Chen, Optical and Photoacoustic Dual-Modality Imaging Guided Synergistic Photodynamic/Photothermal Therapies, *Nanoscale*, 2015, **00**, 1–7.

9 Y. Wang, N. Gong, Y. Li, Q. Lu, X. Wang and J. Li, Atomic-Level Nanorings (A-NRs) Therapeutic Agent for Photoacoustic Imaging and Photothermal/Photodynamic Therapy of Cancer, *J. Am. Chem. Soc.*, 2020, **142**, 1735–1739.
10 J. Wang, L. Zhang, M. Chen, S. Gao and L. Zhu, Activatable Ferritin Nanocomplex for Real-Time Monitoring of Caspase-3 Activation during Photodynamic Therapy, *ACS Appl. Mater. Interfaces*, 2015, **7**, 23248–23256.
11 X. Lin, J. Xie, G. Niu, F. Zhang, H. Gao, M. Yang, Q. Quan, M. A. Aronova, G. Zhang, S. Lee, R. Leapman and X. Chen, Chimeric Ferritin Nanocages for Multiple Function Loading and Multimodal Imaging, *Nano Lett.*, 2011, **11**, 814–819.
12 Z. Zhen, W. Tang, H. Chen, X. Lin, T. Todd, G. Wang, T. Cowger, X. Chen and J. Xie, RGD-Modified Apoferritin Nanoparticles for Efficient Drug Delivery to Tumors, *ACS Nano*, 2013, **7**, 4830–4837.
13 A. F. Breen, G. Wells, L. Turyanska and T. D. Bradshaw, Development of novel apoferritin formulations for antitumour Benzothiazoles, *Cancer Rep.*, 2019, **2**, 1–7.
14 K. Bouzinab, H. S. Summers, M. F. G. Stevens, C. J. Moody, N. R. Thomas, P. Gershkovich, N. Weston, M. B. Ashford, T. D. Bradshaw and L. Turyanska, Delivery of Temozolomide and N3-Propargyl Analog to Brain Tumors Using an Apoferritin Nanocage, *ACS Appl. Mater. Interfaces*, 2020, **12**, 12609–12617.
15 L. Pan, J. Liu and J. Shi, Nuclear-Targeting Gold Nanorods for Extremely Low NIR Activated Photothermal Therapy, *ACS Appl. Mater. Interfaces*, 2017, **9**, 15952–15961.
16 X. Li, L. Xing, K. Zheng, P. Wei, L. Du, M. Shen and X. Shi, Formation of Gold Nanostar-Coated Hollow Mesoporous Silica for Tumor Multimodality Imaging and Photothermal Therapy, *ACS Appl. Mater. Interfaces*, 2017, **9**, 5817–5827.
17 S. R. Panikkanvalappil, N. Hooshmand and M. A. El-Sayed, Intracellular Assembly of Nuclear-Targeted Gold Nanosphere Enables Selective Plasmonic Photothermal Therapy of Cancer by Shifting Their Absorption Wavelength toward Near-Infrared Region, *Bioconjugate Chem.*, 2017, **28**, 2452–2460.
18 L. J. Chen, S. K. Sun, Y. Wang, C. X. Yang, S. Q. Wu and X. P. Yan, Activatable Multifunctional Persistent Luminescence Nanoparticle/Copper Sulfide Nanoprobe for in Vivo Luminescence Imaging Guided Photothermal Therapy, *ACS Appl. Mater. Interfaces*, 2016, **8**, 32667–32674.
19 N. Li, Q. Sun, Z. Yu, X. Gao, W. Pan, X. Wan and B. Tang, Nuclear-Targeted Photothermal Therapy Prevents Cancer Recurrence with NearInfrared Triggered Copper Sulfide Nanoparticles, *ACS Nano*, 2018, **12**, 5197–5206.
20 D. Wang, H. Dong, M. Li, Y. Cao, F. Yang, K. Zhang, W. Dai, C. Wang and X. Zhang, Erythrocyte–Cancer Hybrid Membrane Camouflaged Hollow Copper Sulfide Nanoparticles for Prolonged Circulation Life and Homotypic-Targeting Photothermal/Chemotherapy of Melanoma, *ACS Nano*, 2018, **12**, 5241–5252.
21 Z. Wang, P. Huang, O. Jacobson, Z. Whang, Y. Liu, L. Lin, J. Lin, N. Lu, H. Zhang, R. Tian, G. Niu, G. Liu and X. Chen, Biomineralization-Inspired Synthesis of Copper Sulfide–Ferritin Nanocages as Cancer Theranostics, *ACS Nano*, 2016, **10**, 3453–3460.
22 M. K. Kuimova, M. Bhatti, M. Deonarain, G. Yahioglu, J. A. Levitt, I. Stamati, K. Suhling and D. Phillips, Fluorescence characterisation of multiply-loaded anti-HER2 single chain Fv-photosesitizer conjugates suitable for photodynamic therapy, *Photochem. Photobiol. Sci.*, 2007, **6**, 933–939.
23 M. Michy, T. Massias, C. Bernard, L. Vanwonterghem, M. Henry, M. Guidetti, G. Royal, J. L. Coll, I. Texier, V. Josserand and A. Hurbin, Verteporfin-Loaded Lipid Nanoparticles Improve Ovarian Cancer Photodynamic Therapy In Vitro and In Vivo, *Cancers*, 2019, **11**, 1–19.
24 Y. Mae, T. Kanda, T. Sugihara, T. Takata, H. Kinoshita, T. Sakaguchi, T. Hasegawa, R. Tarumoto, M. Edano, H. Kurumi, Y. Ikebuchi, K. Kawaguchi and H. Isomoto, Verteporfin-photodynamic therapy is effective on gastric cancer cells, *Mol. Clin. Oncol.*, 2020, **13**, 1–6.
25 J. Kim, Y. U. Jo and K. Na, Photodynamic therapy with smart nanomedicine, *Arch. Pharmacal Res.*, 2020, **43**, 22–31.
26 O. Erel, A new automated colorimetric method for measuring total oxidant status, *Clin. Biochem.*, 2005, **38**, 1103–1111.
27 A. Negoescu, P. Lorimier, F. Labat-Moleur, C. Drouet, C. Robert, C. Guillermet, C. Brambilla and E. Brambilla, In situ apoptotic cell labeling by the TUNEL method: improvement and evaluation of cell preparations, *J. Histochem. Cytochem.*, 1996, **44**, 959–968.
28 M. Azizi, H. Ghourchian, F. Yazdian, S. Bagherifam, S. Bekhradnia and B. Nyström, Anti-cancerous effect of albumin coated silver nanoparticles on MDA-MB 231 human breast cancer cell line, *Sci. Rep.*, 2017, **7**, 5178.
29 S. Chen, S. L. Greasley, Z. Y. Ong, P. Naruphontjirakul, S. J. Page, J. V. Hanna, A. N. Redpath, O. Tsigkou, S. Rankin, M. P. Ryan, A. E. Porter and J. R. Jones, Biodegradable zinc-containing mesoporous silica nanoparticles for cancer therapy, *Mater. Today Adv.*, 2020, **6**, 100066.
30 R. Agabeigi, S. H. Rasta, M. Rahmati-Yamchi, R. Salehi and E. Alizadeh, Novel Chemo-Photothermal Therapy in Breast Cancer Using Methotrexate-Loaded Folic Acid Conjugated Au@SiO2 Nanoparticles, *Nanoscale Res. Lett.*, 2020, **15**, 1–14.
31 S. Gurunathan, J. H. Park, J. W. Han and J. Kim, Comparative assessment of the apoptotic potential of silver nanoparticles synthesized by Bacillus tequilensis and Calocybe indica in MDA-MB-231 human breast cancer cells: targeting p53 for anticancer therapy, *Int. J. Nanomed.*, 2015, **10**, 4203–4223.
32 M. Kressel and P. Groscurth, Distinction of apoptotic and necrotic cell deaths by in situ labeling of fragmented DNA, *Cell Tissue Res.*, 1994, **278**, 549–556.
33 S. S. Unver, D. Saraydin and I. Z. D. Sahin, A study on digital image analysis on acrylamide-derived monomers that cause apoptosis in rat cerebrum, *Microsc. Res. Tech.*, 2020, **83**, 436–445.